

Effect of Analog-to-Digital Converter in Distributed Sampling for Sensor Networks

Sinem Coleri Ergen and Pravin Varaiya
 Email: {csinem,varaiya}@eecs.berkeley.edu

November 11, 2005

Abstract

We address the effect of the errors occurring at the analog-to-digital converter (ADC), from quantization noise, circuit noise, aperture uncertainty and comparator ambiguity, on the accuracy of sensor field reconstruction. We focus on the deterministic oversampling of bandlimited sensor fields in a distributed processing environment. It has previously been shown that Pulse Code Modulation (PCM) style sampling fails to decrease the quantization error above some finite sampling rate. We show that the dither-based scheme, developed to decrease the quantization error, fails to decrease random errors associated with circuit noise, aperture uncertainty and comparator ambiguity. We propose an advanced dither-based sampling scheme with the goal of reducing both kinds of errors by increasing the density of the sensor nodes. It is based on distributing the task of improving the quantization error and random error among the nodes. The error of the scheme is shown to be $O(\frac{1}{r^{1/2}})$ for oversampling rate r . We also define the measure of efficiency as the maximum energy consumption in a node per bit gain and show that the proposed scheme has measure of efficiency $O(1)$. Finally, the bit rate of the scheme is $O(\frac{1}{r^{1/2} \log(r)})$ and it offers robustness to node failures in terms of a graceful degradation of reconstruction error.

1 Introduction

Figure 1 illustrates a system for reconstructing sensor field $F(x, y, z, t)$ based on the quantized samples at L sensor nodes. Each node i samples and quantizes the sensor field at location (x_i, y_i, z_i) . The quantized samples are then sent over the communication channel, which may have multiple hops, to a central controller. The central controller finally reconstructs the field. Increasing the density of the nodes in this sensor network setting is expected to improve the accuracy of the reconstructed sensor field. However, if all the error sources are not taken into consideration, the configuration of the nodes may fail to provide any improvement above some density. This paper focuses on the accuracy of the sensor field reconstruction based on the quantized samples of the sensor nodes by considering all types of errors occurring at the analog-to-digital converter (ADC) for bandlimited sensor fields. Most physical signals are approximately bandlimited so can be

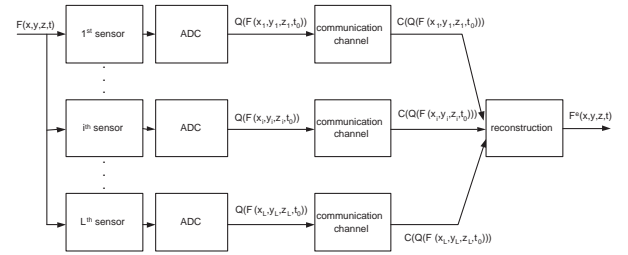


Figure 1: System for reconstructing sensor field.

reconstructed in a stable manner from the samples taken slightly above the Nyquist rate on a uniform lattice. In practice however the errors occurring in the ADC, namely quantization noise, circuit noise, aperture uncertainty and comparator ambiguity, cause unavoidable signal reconstruction errors. The only error mechanism present in an ideal ADC is quantization. This error arises in the transformation of the analog input signal that may assume any value within the input range of the ADC into finite precision output data. In physical ADC devices, on the other hand, there are additional error mechanisms. Aperture uncertainty comes about because an ADC does not sample the input signal at the precise sampling time and location. Comparator ambiguity is due to the finite speed with which transistors in the comparator are able to respond to a small voltage difference.

Previous studies [2, 10, 4, 8, 1] have focused on two sampling schemes to reduce quantization error via oversampling in ADCs: Pulse Code Modulation (PCM) style sampling and dither-based sampling scheme. In PCM style sampling, the signal is sampled regularly at constant period τ and then quantized with a step q . Then the signal is reconstructed by low-pass filtering the sequence of quantized samples with cut-off frequency equal to the signal bandwidth. In [2], it is shown that the quantization error in this sampling scheme can be modelled as a white noise independent of the input if the quantization step is small enough and a sufficiently large number of quantization levels is available. According to the white noise model, the conversion accuracy improves in proportion to the sampling interval τ . In [10], however, it is shown that the accuracy improvement by a factor τ is valid only in a small range of parameters q and τ and the error does not tend to zero as τ decreases but reaches a floor level for some finite τ . This

is reasonable since the quantization error becomes correlated as τ decreases.

To improve the quantization error, a dither-based sampling scheme has recently been proposed. Dither-based sampling is based on recording positions of quantization threshold crossings of the input signal added to a deterministic dither function. [4] shows that the conversion accuracy improves in proportion to τ^2 . Moreover, representing quantization threshold crossing requires only a logarithmic increase of the bit rate in contrast to PCM style sampling scheme.

The above schemes assume an ideal ADC so only quantization error is present. It is not clear however how other sources of errors affect the reconstruction performance. This paper aims to describe and analyze the effect of these random error sources in more detail. We show that a dither based scheme is successful at decreasing the quantization error by increasing the sampling rate but fails to eliminate random errors. On the other hand, PCM style sampling scheme fails to eliminate quantization error when the sampling interval decreases to a certain value but succeeds in decreasing random error as the oversampling rate increases. We propose an advanced dither based scheme that is successful at eliminating both quantization and random errors by combining PCM-style and dither-based schemes.

The rest of the paper is as follows. Section 2 gives the system model and explains PCM-style and dither based sampling schemes together with their quantization performance. Section 3 inspects random error sources and analyzes the performance of these two systems in reducing their effect on the signal reconstruction accuracy. Section 4 proposes a new sampling scheme to reduce both quantization and random errors. Section 5 analyzes the trade-off between accuracy and energy consumption in the proposed sampling scheme together with the earlier ones. Sections 6 and 7 describes the bit rate to the central processor and robustness of the scheme to node failures respectively. Section 8 concludes the paper.

2 System Model

The analysis of the sampling schemes is performed for 1-D spatially bandlimited sensor field at a certain time t_0 . This field is represented by $f(x) = F(x, y_0, z_0, t_0)$ for the rest of the paper. Without loss of generality, the field $f(x)$ is assumed to belong to the set \mathcal{C} , the set of π -bandlimited signals with finite energy and amplitude smaller than 1, $\mathcal{C} = \{f : f \in L^2(\mathbb{R}), \|f\|_\infty \leq 1, \hat{f}(w) = 0, |w| > \pi\}$, where \hat{f} denotes the Fourier transform of f .

The Nyquist period for $f(x)$ is $T_{NQ} = 1$. The sampling rate is assumed to be $\lambda \geq 1$. The PCM-style and dither-based sampling schemes together with their quantization error performance are summarized in Sections 2.1 and 2.2 respectively.

2.1 PCM-Style Sampling Scheme

In PCM-style sampling scheme, the signal $f(x)$ is reconstructed from the samples at regular intervals $\tau = \frac{1}{\lambda}$, $\{f(\frac{n}{\lambda})\}_{n \in \mathbb{Z}}$, with k -bit quantizer.

Proposition 1: [7] For each $\lambda \geq 1$, there exists a $\lambda\pi$ -bandlimited kernel $g(x)$ such that $C_\lambda = \sup_{x \in \mathbb{R}} (\sum_n |g(x - \frac{n}{\lambda})|^2) < \infty$ and

$$f(x) = \frac{1}{\lambda} \sum_n f(\frac{n}{\lambda}) g(x - \frac{n}{\lambda}), \forall x \in \mathbb{R} \quad (1)$$

An example g is such that $|\hat{g}(w)| = 0$ for $|w| > \lambda\pi$, $\hat{g}(w) = \frac{1}{\sqrt{2\pi}}$ for $|w| \leq \pi$ and $0 < \hat{g}(w) < \frac{1}{\sqrt{2\pi}}$ for $\pi < |w| < \lambda\pi$.

K -bit quantization perturbs the samples $f(\frac{n}{\lambda})$ by ϵ_n such that $\tilde{f}(\frac{n}{\lambda}) = f(\frac{n}{\lambda}) + \epsilon_n$, in which $|\epsilon_n| \leq 2^{-k}$. In [2], it is shown that the quantization error can be modelled as a white noise independent of the input if the quantization step is small enough and a sufficiently large number of quantization levels is available. According to the white noise model, the reconstructed mean-square error is upper-bounded as

$$E(|f(x) - \frac{1}{\lambda} \sum_n \tilde{f}(\frac{n}{\lambda}) g(x - \frac{n}{\lambda})|^2) \leq C_\lambda 2^{-2k} \tau^2. \quad (2)$$

For $g(x) = \text{sinc}(x)$, the upper bound is $2^{-2k} \tau$.

However, the white noise model is not asymptotically valid and experimental results in [10] demonstrate that for high oversampling ratios the error decay rate of the reconstruction is lower than that implied by the white noise model since the quantization error becomes correlated. The error does not tend to zero as the oversampling rate increases but reaches a floor level for some finite rate. Therefore, the PCM-style sampling is not successful at decreasing the quantization error when the oversampling rate is above a certain value.

2.2 Dither-based Sampling Scheme

Dither-based sampling is based on recording the position of the quantization threshold crossings of the function $f(x)$ added to a deterministic dither function $d_b(x)$ for b -bit quantizer and rate $\lambda > 1$. The goal of the dither function $d_b(x)$ is to guarantee that $f(x) + d_b(x)$ has a quantization threshold crossing in each interval $(\frac{n}{\lambda}, \frac{n+1}{\lambda})_{n \in \mathbb{Z}}$. The number of nodes inside each of these intervals then determines the sampling interval τ so how accurate the location of these crossings can be found.

Figure 2 shows an example of 1-bit dither sampling for sampling intervals $\tau = \frac{1}{4\lambda}$ and $\tau = \frac{1}{8\lambda}$ in parts a) and b) respectively. The arrows show the locations after which there is a threshold crossing within τ interval.

Let x_n be the estimated threshold crossing inside interval $(\frac{n}{\lambda}, \frac{n+1}{\lambda})$ for $n \in \mathbb{Z}$. The sequence $\{x_n\}_{n \in \mathbb{Z}}$ is uniformly discrete, i.e. $\inf_{n, k \in \mathbb{Z}, n \neq k} |x_n - x_k| > 0$. Since the lower uniform density of $\{x_n\}_{n \in \mathbb{Z}}$ is equal to $\lambda > 1$, it constitutes a stable sampling, i.e. $f(x)$ can be perfectly recovered from $\{f(x_n)\}_{n \in \mathbb{Z}}$ provided they are exactly accurate [5]. The effect of the estimation error in $f(x_n)$ on the reconstruction accuracy is now briefly explained first for 1-bit then for b -bit dithered scheme.

The goal of the dither function in 1-bit dithered scheme is to guarantee that $f(x) + d_1(x)$ has a zero-crossing in each interval $(\frac{n}{\lambda}, \frac{n+1}{\lambda})_{n \in \mathbb{Z}}$. The dither function design has been explained in more detail in [8]. An example appropriate dither is the sine function, $d(t) = \gamma \sin(\lambda\pi t)$ where $\gamma > 1$.

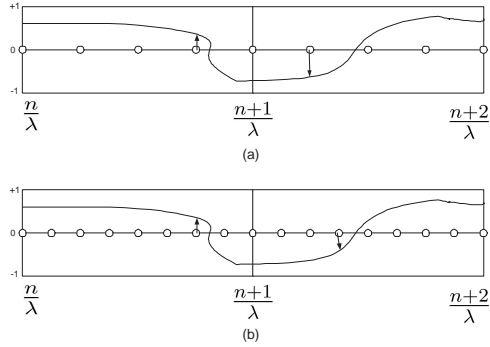


Figure 2: Dither based sampling for a) $\tau = \frac{1}{4\lambda}$ b) $\tau = \frac{1}{8\lambda}$

2^k nodes with 1-bit ADCs are placed uniformly in each interval $(\frac{n}{\lambda}, \frac{n+1}{\lambda})$ to record the sign of the dithered signal $f(x) + d_1(x)$ so the sampling interval $\tau = \frac{1}{\lambda 2^k}$. Let $m_n \in [0, 2^k - 1]$ be the smallest index for which $[f + d_1](\frac{n}{\lambda} + m_n \tau)$ and $[f + d_1](\frac{n}{\lambda} + (m_n + 1)\tau)$ have opposite signs. Then from the intermediate value theorem, $f(z_n) + d_1(z_n) = 0$ at some point $z_n \in (\frac{n}{\lambda} + m_n \tau, \frac{n}{\lambda} + (m_n + 1)\tau)$. For $x_n = m_n + \frac{1}{2}$, $|[f + d_1](z_n) - [f + d_1](\frac{n}{\lambda} + x_n \tau)| \leq (\pi + \Delta)|z_n - \frac{n}{\lambda} - x_n \tau|$ so

$$|f(\frac{n}{\lambda} + x_n \tau) - (-d_1(\frac{n}{\lambda} + x_n \tau))| \leq (\pi + \Delta) \frac{\tau}{2}. \quad (3)$$

Proposition 2: [4] Suppose $\inf_{j,l \in \mathbb{Z}, j \neq l} |t_j - t_l| > 0$ and $\sup_{n \in \mathbb{Z}} |t_n - \frac{n}{\lambda}| < \infty$, where $\lambda > 1$. Then there exist interpolating functions ψ_n with $C' = \sup_{x \in \mathbb{R}} \sum_{n \in \mathbb{Z}} |\psi_n(x - t_n)| < \infty$ such that for any π -bandlimited function $f(x)$,

$$f(x) = \sum_n f(t_n) \psi_n(x - t_n) \quad (4)$$

where ψ_n and C' do not depend on f . ψ_n are the functions associated with the sequence $(t_n)_{n \in \mathbb{Z}}$.

By using this proposition with $t_n = \frac{n}{\lambda} + x_n \tau$, one can reconstruct an approximation \tilde{f} for f as

$$\tilde{f}(x) = - \sum_n d_1(t_n) \psi_n(x - t_n). \quad (5)$$

Then the error between f and \tilde{f} is

$$|\tilde{f}(x) - f(x)| \leq C'(\pi + \Delta) \frac{\tau}{2}, \quad (6)$$

so the mean square-error is

$$E(|\tilde{f}(x) - f(x)|^2) \leq C(\pi + \Delta)^2 \tau^2, \quad (7)$$

where $C = \frac{C'^2}{4}$.

PCM-style sampling uses k -bit ADC at one location in each interval of length $\frac{1}{\lambda}$ whereas 1-bit dithered sampling uses 1-bit ADCs at 2^k locations uniformly distributed at intervals of length $\tau = \frac{1}{2^k \lambda}$. From the ‘‘conservation of bits’’ principle described in [8], for $1 \leq b \leq k$, there exists a dither-based sampling scheme with not more than 2^{k-b+1} , b -bit ADCs in each interval $(\frac{n}{\lambda}, \frac{n+1}{\lambda})_{n \in \mathbb{Z}}$ achieving a worst-case reconstruction accuracy of the order of 2^{-k} .

In the proposed sampling and quantization scheme developed in [8], 2^{k-b+1} , b -bit ADCs are placed at locations $\{\frac{n}{\lambda} + m\tau\}$ for $m = 0, \dots, 2^{k-b+1} - 1$ and $n \in \mathbb{Z}$, $\tau = \frac{1}{\lambda 2^k}$. The dither function $d_b(x)$ is designed such that the sum $f(x) + d_b(x)$ crosses some level in every interval of form $[A_n, B_n] = [\frac{n}{\lambda}, \frac{n}{\lambda} + (2^{k-b+1} - 1)\tau]$ [8].

Let $m_n \in [0, 2^{k-b+1} - 1]$ be the smallest index for which $[f + d_b](\frac{n}{\lambda} + m_n \tau)$ and $[f + d_b](\frac{n}{\lambda} + (m_n + 1)\tau)$ are on opposite sides of a quantization threshold $l_n \in \{0, \mp \frac{1}{2^{b-1}}, \dots, \mp (1 - \frac{1}{2^{b-1}})\}$. Then from the intermediate value theorem, $f(z_n) + d_b(z_n) = l_n$ at some point $z_n \in (\frac{n}{\lambda} + m_n \tau, \frac{n}{\lambda} + (m_n + 1)\tau)$. For $x_n = m_n + \frac{1}{2}$, $|[f + d_b](z_n) - [f + d_b](\frac{n}{\lambda} + x_n \tau)| \leq (\pi + \Delta_b)|z_n - \frac{n}{\lambda} - x_n \tau|$ so

$$|f(\frac{n}{\lambda} + x_n \tau) - (l_n - d_b(\frac{n}{\lambda} + x_n \tau))| \leq (\pi + \Delta_b) \frac{\tau}{2}. \quad (8)$$

By using Proposition 2 with $t_n = \frac{n}{\lambda} + x_n \tau$, one can reconstruct an approximation \tilde{f} for f as

$$\tilde{f}(x) = \sum_n (l_n - d_b(t_n)) \psi_n(x - t_n). \quad (9)$$

Then the mean square-error between f and \tilde{f} is

$$E(|\tilde{f}(x) - f(x)|^2) \leq C(\pi + \Delta_b)^2 \tau^2. \quad (10)$$

This means that in contrast to PCM-style sampling, b -bit dithered scheme is able to decrease the mean square quantization error proportionally to τ^2 .

3 Random Error Sources

Previous work on sampling schemes have assumed an ideal ADC so only the effect of quantization error on the reconstruction accuracy is considered. Over the last decade however the voltage levels of the circuits have decreased for low-power operation. This decrease together with the improvement in the quantization error requires considering the effect of random error sources on the reconstruction of the sensor field. Random error sources are given as follows [11]:

- **Circuit noise:** The circuit noise observed at the ADC input consists of various components such as device noise, conducted noise and radiated noise. Device noise comes from devices like amplifiers and resistors that cannot work effectively in the ADC. Usually, these devices are chosen for specifications that are unrelated to noise. Another area that contributes to circuit noise is conducted noise. The origin of conducted noise is either device noise or emitted noise. It can come from the devices in the analog signal path as well as the power supply devices. For instance, a switched-mode power supply creates supply noise, which is injected into the sensitive analog devices. A third source of error is radiated noise. Commonly, this noise can occur because of the coupling of signals from two traces that are parallel and in close proximity. Radiated noise can also come from external electromagnetic interference signals. Circuit noise is usually modelled as an additive zero mean white Gaussian noise with standard deviation much smaller than the dynamic range of the signal.

- **Aperture uncertainty:** In a system where each sample is taken at the same sensor node, aperture uncertainty results since the time difference between sampling events fluctuates due to a combination of timing jitter and skew in the mechanism or clock that triggers sampling. The same effect occurs in the spatial sampling because the ADC in different sensors do not sample the input signal at the expected precise location and time. The error in location comes from the imperfect spatial localization of the sensor nodes whereas the error in time results from the synchronization error of the sensor nodes. Let (x_i, y_i, z_i) and t_0 be the location and time node i should be sampled and (x'_i, y_i, z_i) and t'_0 be the real location and time node i is sampled. The aperture uncertainty is

$$F(x'_i, y_i, z_i, t'_0) - F(x_i, y_i, z_i, t_0). \quad (11)$$

The mean difference is expected to be zero.

- **Comparator ambiguity:** This effect is due to the finite speed of integrated circuit technology being used. The comparators in an ADC have limited ability of resolving an input voltage in a certain amount of time due to the finite transistor speed. This leads to a trade-off between the sampling rate in time and maximum possible resolution of the ADC converter. Based on the assumption that the sampling rate in time is fixed, the comparator ambiguity has the same distribution for any spatial sampling rate. Since the effect of the comparator ambiguity depends on the ADC design, which may be parallel comparator, successive approximation, counting or delta-modulation type, it is usually either ignored or included inside the circuit noise as an additive white Gaussian noise.

Without loss of generality, we assume that the sum of all these errors has mean zero. Furthermore, the error at each spatial sampling point is expected to be independent with the same distribution $p(v)$. Let the variance of $p(v)$ be σ^2 . Notice that we don't assume any specific distribution.

We assume that the quantization error and the random error are additive. This system then becomes very similar to non-subtractively dithered systems. In [9], it has been shown that the moments of the total error can be made independent of the system input signal and of one another by carefully choosing the distribution of the random error. However, in ADC, the distribution of the random error is not known and cannot be controlled. Next, we analyze the effect of the random error on PCM-style and dither-based sampling schemes in Sections 3.1 and 3.2.

3.1 PCM-Style Sampling Scheme

The samples $f(\frac{n}{\lambda})$ are perturbed by an additional error μ_n such that $\tilde{f}(\frac{n}{\lambda}) = f(\frac{n}{\lambda}) + \epsilon_n + \mu_n$, where μ_n has mean zero and variance σ^2 , and μ_i and μ_j are independent for $i \neq j$. The reconstructed

mean-square error is as follows:

$$E(|f(x) - \frac{1}{\lambda} \sum_n \tilde{f}(\frac{n}{\lambda})g(x - \frac{n}{\lambda})|^2) \quad (12)$$

$$= E(|\frac{1}{\lambda} \sum_n (\mu_n + \epsilon_n)g(x - \frac{n}{\lambda})|^2) \quad (13)$$

$$= E(\frac{1}{\lambda^2} |\sum_n \mu_n g(x - \frac{n}{\lambda})|^2) \quad (14)$$

$$+ E(\frac{1}{\lambda^2} |\sum_n \epsilon_n g(x - \frac{n}{\lambda})|^2)$$

$$+ E(\frac{2}{\lambda^2} \sum_m \mu_m g(x - \frac{m}{\lambda}) \sum_n \epsilon_n g(x - \frac{n}{\lambda}))$$

The first term is equal to

$$E(\frac{1}{\lambda^2} |\sum_n \mu_n g(x - \frac{n}{\lambda})|^2) = \frac{\sigma^2}{\lambda^2} \sum_n |g(x - \frac{n}{\lambda})|^2 \quad (15)$$

For $g(x) = \text{sinc}(x)$, the mean-square random error is equal to $\frac{\sigma^2}{\lambda}$. The effect of random error sources therefore decreases as the sampling rate λ increases.

The second and third terms on the other hand correspond to the quantization error and the cross correlation of quantization error and random error. In Section 2.1, we have seen that the second term does not tend to zero as the oversampling rate increases but reaches a floor level for some finite rate so is the bottleneck in PCM-style sampling.

3.2 Dither-based Sampling Scheme

The goal of the dither function $d_b(x)$ in dither-based sampling scheme is to guarantee at least one crossing of a quantization threshold in each interval $(\frac{n}{\lambda}, \frac{n+1}{\lambda})$ for $n \in \mathbb{Z}$. The only way to provide this guarantee is to constrain the sum of the signal $f(x)$ and the random noise $e(x)$ at each location x to have a limited dynamic range.

We have seen that circuit noise is usually modelled as an additive zero mean white Gaussian noise with standard deviation much smaller than the dynamic range of the signal. For a variance σ^2 , the probability that the circuit noise is more than 6σ is smaller than 10^{-9} . We can therefore assume that the circuit noise has a maximum magnitude of 6σ .

Comparator ambiguity can also be upper-bounded for bandlimited signals. Since $F(x, y, z, t)$ is bandlimited, there exists u_s and u_t so that:

$$1. |F'(x, y_i, z_i, t_0)| < u_s, \forall \text{ node } i$$

$$2. |F'(x_i, y_i, z_i, t)| < u_t, \forall \text{ node } i$$

which results in:

$$1. |F(x'_i, y_i, z_i, t_0) - F(x_i, y_i, z_i, t_0)| < u_s |x'_i - x_i|, \forall \text{ node } i$$

$$2. |F(x_i, y_i, z_i, t'_0) - F(x_i, y_i, z_i, t_0)| < u_t |t'_0 - t_0|, \forall \text{ node } i$$

Then if the misplacement and synchronization error is upper-bounded by m_s and m_t respectively, the resulting error in the sample due to aperture uncertainty is upper-bounded;

$$\begin{aligned} & |F(x'_i, y_i, z_i, t'_0) - F(x_i, y_i, z_i, t_0)| \\ & \leq u_s |x'_i - x_i| + u_t |t'_0 - t_0| \leq u_s m_s + u_t m_t. \end{aligned} \quad (16)$$

The error $e(x)$ at location x has mean 0, variance σ^2 and has a limited dynamic range such that

$$|f(x) + e(x)| < (1 + U). \quad (17)$$

The dither function $d_{b,e}(x)$ is then designed so that the sum $f(x) + e(x) + d_{b,e}(x)$ crosses some level in every interval of form $[A_n, B_n] = [\frac{n}{\lambda}, \frac{n}{\lambda} + (2^{k-b+1} - 1)\tau]$ for $n \in \mathbb{Z}, \lambda > 1$. Since $|f(x) + e(x)| < (1 + U)$, this is satisfied if the function $d_{b,e}$ is designed by normalizing d_b by $1 + U$. We omit the details due to space constraints.

Let $m_n \in [0, 2^{k-b+1} - 1]$ be the smallest index for which $[f + e + d_{b,e}](\frac{n}{\lambda} + m_n \tau)$ and $[f + e + d_{b,e}](\frac{n}{\lambda} + (m_n + 1)\tau)$ are on opposite sides of a quantization threshold $l_n \in \{0, \mp \frac{1}{2^{b-1}}, \dots, \mp(1 - \frac{1}{2^{b-1}})\}$. From the intermediate value theorem, $f(z_n) + e(z_n) + d_{b,e}(z_n) = l_n$ at some point $z_n \in (\frac{n}{\lambda} + m_n \tau, \frac{n}{\lambda} + (m_n + 1)\tau)$. For $x_n = m_n + \frac{1}{2}$,

$$\begin{aligned} & [f + e + d_{b,e}](z_n) - [f + d_{b,e}](\frac{n}{\lambda} + x_n \tau) \\ & = (l_n - d_{b,e}(\frac{n}{\lambda} + x_n \tau)) - f(\frac{n}{\lambda} + x_n \tau), \end{aligned} \quad (18)$$

where the error corresponding to quantization and random error are $q_n = [f + d_{b,e}](z_n) - [f + d_{b,e}](\frac{n}{\lambda} + x_n \tau)$ and $e_n = e(z_n)$ respectively.

By using Proposition 2 with $t_n = \frac{n}{\lambda} + x_n \tau$, one can reconstruct an approximation \tilde{f} for f as

$$\tilde{f}(x) = \sum_n (l_n - d_{b,e}(t_n)) \psi_n(x - t_n) \quad (19)$$

Then the mean square-error between f and \tilde{f} is

$$E(|\tilde{f}(x) - f(x)|^2) \quad (20)$$

$$= E(|\sum_n (f(t_n) - (l_n - d_{b,e}(t_n))) \psi_n(x - t_n)|^2) \quad (21)$$

$$= E(|\sum_n (q_n + e_n) \psi_n(x - t_n)|^2) \quad (22)$$

$$= E(|\sum_n q_n \psi_n(x - t_n)|^2) + E(|\sum_n e_n \psi_n(x - t_n)|^2) \quad (23)$$

$$\begin{aligned} & + E(\sum_m q_m \psi_m(x - t_m) \sum_n e_n \psi_n(x - t_n)) \\ & \leq C(\pi + \Delta_{b,e})^2 \tau^2 + \sigma^2 \sum_n |\psi_n(x - t_n)|^2 \end{aligned} \quad (24)$$

$$\begin{aligned} & + C'(\pi + \Delta_{b,e}) \frac{\tau}{2} E(|\sum_n e(z_n) \psi_n(x - t_n)|) \\ & \leq C(\pi + \Delta_{b,e})^2 \tau^2 + C'^2 \sigma^2 + C''(\pi + \Delta_{b,e}) \tau, \end{aligned} \quad (25)$$

where $C'' = C'^2 \frac{E(|e(z_n)|)}{2}$. This shows that although dither-based sampling scheme is successful at decreasing quantization error by increasing oversampling rate λ , it cannot decrease the random error.

4 Redundant Dither-Based Sampling Scheme

In Section 3, we observed that PCM-style sampling scheme is successful at decreasing random error whereas dither-based scheme decreases quantization error. In PCM-style sampling, the quantization error does not tend to zero as the oversampling rate increases but reaches a floor level for some finite rate. On the other hand, random error cannot be eliminated in dither-based sampling scheme due to the lack of diversity. This section introduces a redundant dither-based scheme that aims at decreasing the effect of both quantization and random error effect.

In PCM style sampling, the decrease in sampling interval τ corresponds to taking more samples of $f(x)$. In dither-based scheme on the other hand the sampling rate λ is fixed. The decrease in sampling interval corresponds to finding the value of the sample with higher accuracy. Therefore, the dither-based scheme can be thought of a spatial quantizer that improves quantization error performance whereas PCM-style sampling provides more samples so more diversity to decrease random errors. It is possible to decrease both kinds of errors by distributing the task of improving the quantization error and random error among the sensor nodes.

Let us assume that each sensor node has a b -bit ADC. Let us call $\lambda > 1$ as the sampling rate and r as the oversampling rate. Let the number of nodes inside each interval of length $\frac{1}{\lambda}$ be given by $r = r_1 r_2$ where $r_2 = 2^{k_2 - b + 1}, k_2 \geq b - 1$. The placement of the nodes is as follows:

- Divide each interval of length $\frac{1}{\lambda}$ into r_1 equal intervals.
- Place r_2 , b -bit ADCs at locations $\{\frac{n}{r_1 \lambda} + m \tau\}$ for $m = 0, 1, \dots, r_2 - 1$, and $n \in \mathbb{Z}, \tau = \frac{1}{r_1 r_2 \lambda 2^{b-1}}$
- Design dither function $d_{b,r_1,r_2}(x)$ so that the sum $f(x) + e(x) + d_{b,r_1,r_2}(x)$ crosses some level in every interval of the form $[A_n, B_n] = [\frac{n}{r_1 \lambda}, \frac{n}{r_1 \lambda} + (r_2 - 1)\tau]$.
- Send the level crossing inside each interval $[A_n, B_n]$ to the central controller for reconstruction.
- Central controller estimates $\tilde{f}_i(x)$ from the threshold crossings in intervals $[\frac{n}{\lambda} + i \frac{1}{r_1 \lambda}, \frac{n}{\lambda} + (i + 1) \frac{1}{r_1 \lambda}]_{n \in \mathbb{Z}}$ for $i = 0, 1, \dots, r_1 - 1$. Estimate of $f(x)$ is then given by $\tilde{f}(x) = \frac{\sum_{i=0}^{r_1-1} \tilde{f}_i(x)}{r_1}$.

Notice that dither-based scheme corresponds to $r_1 = 1$.

Let $m_n^i \in [0, r_2 - 1]$ be the smallest index for which $[f + e + d_{b,e}](\frac{n}{\lambda} + i \frac{1}{r_1 \lambda} + m_n^i \tau)$ and $[f + e + d_{b,e}](\frac{n}{\lambda} + i \frac{1}{r_1 \lambda} + (m_n^i + 1)\tau)$ are on opposite sides of a quantization threshold $l_n^i \in \{0, \mp \frac{1}{2^{b-1}}, \dots, \mp(1 - \frac{1}{2^{b-1}})\}$. From the intermediate value theorem, $f(z_n^i) + e(z_n^i) + d_{b,e}(z_n^i) = l_n^i$ at some point $z_n^i \in (\frac{n}{\lambda} + i \frac{1}{r_1 \lambda} + m_n^i \tau, \frac{n}{\lambda} + i \frac{1}{r_1 \lambda} + (m_n^i + 1)\tau)$. For $x_n^i = m_n^i + \frac{1}{2}$,

$$\begin{aligned} & [f + e + d_{b,e}](z_n^i) - [f + d_{b,e}](\frac{n}{\lambda} + x_n^i \tau) \\ & = (l_n^i - d_{b,e}(\frac{n}{\lambda} + x_n^i \tau)) - f(\frac{n}{\lambda} + x_n^i \tau), \end{aligned} \quad (26)$$

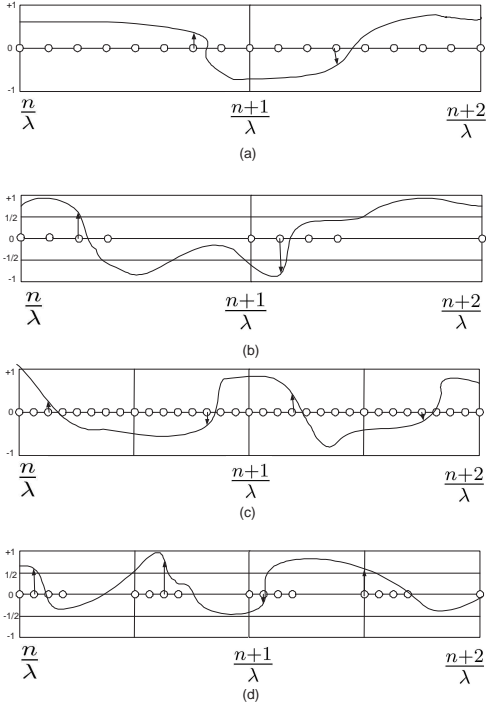


Figure 3: Sampling schemes for dither-based sampling (a) and b)) and advanced dither-based sampling (c) and d)). a) $r_1 = 1, r_2 = 8, b = 1$ b) $r_1 = 1, r_2 = 4, b = 2$ c) $r_1 = 2, r_2 = 8, b = 1$ d) $r_1 = 2, r_2 = 4, b = 2$

where the error corresponding to quantization and random error are $[f + d_{b,e}](z_n^i) - [f + d_{b,e}](\frac{n}{\lambda} + x_n^i \tau)$ and $e(z_n^i)$ respectively.

For $t_n^i = \frac{n}{\lambda} + x_n^i \tau$, one can reconstruct an approximation \tilde{f}_i for f as

$$\tilde{f}_i(x) = \sum_n (l_n^i - d_{b,e}(t_n^i)) \psi_n^i(x - t_n^i) \quad (27)$$

$$(28)$$

Figure 3 illustrates the advanced dither-based scheme together with the dither-based scheme.

Theorem 1: For the scheme above, the mean-square error is

$$E(|\tilde{f}(x) - f(x)|^2) \leq C_1 \frac{1}{r_2^2} + C_2 \frac{\sigma^2}{r_1} + C_3 \frac{1}{r_2}, \quad (29)$$

for some constants C_1, C_2 and C_3 .

Proof: We first make some definitions. Let the quantization error in the estimation $\tilde{f}_i(x)$ be given by $q_i(x)$,

$$q_i(x) = \sum_n ([f + d_{b,e}](z_n^i) - [f + d_{b,e}](\frac{n}{\lambda} + x_n^i \tau)) \psi_n^i(x - t_n^i) \quad (30)$$

Let the random error in the estimation $\tilde{f}_i(x)$ be given by $e_i(x)$,

$$e_i(x) = \sum_n e(z_n^i) \psi_n^i(x - t_n^i). \quad (31)$$

Then the error introduced in $\tilde{f}_i(x)$ is

$$\tilde{f}_i(x) - f(x) = e_i(x) + q_i(x). \quad (32)$$

The mean square error between f and \tilde{f} is

$$E(|\tilde{f}(x) - f(x)|^2) \quad (33)$$

$$= E(|\frac{\sum_{i=0}^{r_1-1} \tilde{f}_i(x)}{r_1} - f(x)|^2) \quad (34)$$

$$= E(|\frac{\sum_{i=0}^{r_1-1} \tilde{f}_i(x) - f(x)}{r_1}|^2) \quad (35)$$

$$= E(|\frac{\sum_{i=0}^{r_1-1} q_i(x) + e_i(x)}{r_1}|^2) \quad (36)$$

$$= E(|\frac{\sum_{i=0}^{r_1-1} q_i(x)}{r_1}|^2) + E(|\frac{\sum_{i=0}^{r_1-1} e_i(x)}{r_1}|^2) + 2E(\frac{\sum_{i=0}^{r_1-1} q_i(x)}{r_1} \frac{\sum_{j=0}^{r_1-1} e_j(x)}{r_1}). \quad (37)$$

The amplitude constraint on d_{b,r_1,r_2} does not change as a function of r_1 and r_2 but the amplitude change requirement is over an interval $r_2 \tau = \frac{1}{r_1 \lambda 2^{b-1}}$. Therefore, the derivative $\Delta_{b,r_1,r_2} = K r_1 \lambda 2^{b-1}$ for a constant value K . The quantization error is upper-bounded as follows from Sections 2.2 and 3.2:

$$|q_i(x)| \leq C'(\pi + \Delta_{b,r_1,r_2}) \frac{\tau}{2} \quad (38)$$

$$\leq C' r_1 \lambda 2^{b-1} (\pi + K) \frac{1}{r_1 r_2 \lambda 2^b} \quad (39)$$

$$= C \frac{1}{r_2}, \quad (40)$$

where $C = C' \frac{(\pi+K)}{2}$. The inequality 39 comes from the fact that $r_1 \lambda 2^{b-1} \geq 1$.

Then the mean-square quantization error is

$$E(|\frac{\sum_{i=0}^{r_1-1} q_i(x)}{r_1}|^2) \leq E((\frac{\sum_{i=0}^{r_1-1} |q_i(x)|}{r_1})^2) \quad (41)$$

$$\leq (r_1 \frac{C}{r_2})^2 = C^2 \frac{1}{r_2^2}. \quad (42)$$

The mean square random error is

$$E(|\frac{\sum_{i=0}^{r_1-1} e_i(x)}{r_1}|^2) = E(\frac{\sum_{i=0}^{r_1-1} e_i(x)^2}{r_1^2}) \quad (43)$$

$$\leq r_1 C'^2 \sigma^2 \frac{1}{r_1^2} = C'^2 \frac{\sigma^2}{r_1}. \quad (44)$$

The cross correlation of quantization error and random error is

$$E(\frac{\sum_{i=0}^{r_1-1} q_i(x)}{r_1} \frac{\sum_{j=0}^{r_1-1} e_j(x)}{r_1}) \leq \frac{C}{r_2} E(|\frac{\sum_{j=0}^{r_1-1} e_j(x)}{r_1}|) \quad (45)$$

$$\leq C_3 \frac{1}{r_2}, \quad (46)$$

where $C_3 = CE(|e_j|)$.

The upper bound on the mean-square error then follows. \square

Notice that the errors are on the same order if $r_1 = r_2 = r^{1/2}$. Then the error is equal to $\frac{1}{r^{1/2}} (C_1 \frac{1}{r^{1/2}} + C_2 \sigma^2 + C_3)$ so the error is $O(\frac{1}{r^{1/2}})$ for oversampling rate r .

5 Energy-Accuracy Trade-off

We have so far described the error performance of sampling schemes. In this section, we analyze the energy performance of these schemes to understand the trade-off between their accuracy and energy consumption.

For a specific (λ, r_1, r_2) , the nodes are placed at $(\frac{n}{\lambda} + i\frac{1}{r_1\lambda} + j\tau)$ for $n \in \mathbb{Z}, i \in [0, r_1 - 1], j \in [0, r_2 - 1]$, in which $\tau = \frac{1}{r_1 r_2 \lambda 2^{b-1}}$. The measure of efficiency is defined as the maximum energy consumption in a node per bit gain. The bit gain that the scheme provides is defined to be negative of logarithmic decrease in the mean-square error:

$$b_g = -\log(\sup_{x \in \mathbb{R}} E(|\tilde{f}(x) - f(x)|^2)) \quad (47)$$

$$\geq -\log(C_1 \frac{1}{r_2^2} + C_2 \frac{\sigma^2}{r_1} + C_3 \frac{1}{r_2}) \quad (48)$$

The lower bound is equal to $\frac{1}{2} \log(r) - \log(\frac{C_1}{r^{1/2}} + C_2 \sigma^2 + C_3)$ for the case where $r_1 = r_2 = r^{1/2}$. Therefore, the bit gain is $\Omega(\log(r))$.

Let N be the number of periods of length $\frac{1}{\lambda}$ that are monitored by the central controller. The central controller is located at the location of the rightmost sensor node. The task of each node is as follows:

- Determine b -bit quantized value of $f(x) + e(x) + d_{b,r_1,r_2}(x)$ at its location x .
- If the node itself and its left neighbor belong to the same interval $(\frac{n}{\lambda} + i\frac{1}{r_1\lambda} + [0, r_2 - 1]\tau)$ for the same n and i , receive the information about whether a level has been crossed during that interval, which requires 1-bit, and the value of the level at the left neighbor, which requires b bits.
- The nodes at the first level crossing inside the interval $(\frac{n}{\lambda} + i\frac{1}{r_1\lambda} + (m_n^i + 1)\tau)_{n \in [1, N], i \in [0, r_1 - 1]}$ transmit the level crossing information inside their interval to the right according to the forwarding algorithm, which will be described next.
- The nodes forward the level crossing information of the intervals on their right to the left according to the forwarding algorithm.

At each node, the energy is consumed in the sensor, ADC, transmission and reception of packets. Denote the energy consumed in sensor by e_s , in ADC by e_{ADC} , in transmitting a bit over a distance d by $e_t(d)$ and in receiving a bit by e_r . e_s and e_{ADC} do not depend on r_1 and r_2 . The radio spends $e_t(d) = e_{elec} + \epsilon_{amp} d^\alpha$ to transmit 1-bit over a transmission radius of d units whereas the radio spends $e_r = e_{elec}$ to receive 1-bit, where e_{elec} is the electronics energy, ϵ_{amp} is the amplifier energy and α is the attenuation constant.

In determining the level crossing inside each interval $(\frac{n}{\lambda} + i\frac{1}{r_1\lambda} + [0, r_2 - 1]\tau)_{n \in [1, N], i \in [0, r_1 - 1]}$, the node receives and transmits the information about whether a level has been crossed during that interval together with the value of the level at the left neighbor over the distance τ . The first part of energy consumption in a node is then upper bounded as

$$e_1 \leq (b+1)(e_{elec} + \epsilon_{amp} \tau^\alpha + e_{elec}) \quad (49)$$

$$= (b+1)(2e_{elec} + \epsilon_{amp} (\frac{1}{r_1 r_2 \lambda 2^{b-1}})^\alpha). \quad (50)$$

The forwarding algorithm then determines the energy consumption of the scheme. The sensor node at the first level crossing inside each interval, i.e. $(\frac{n}{\lambda} + i\frac{1}{r_1\lambda} + (m_n^i + 1)\tau)_{n \in [1, N], i \in [0, r_1 - 1]}$, has the level crossing information, which should be forwarded to the central controller. The intervals are classified into r_1 groups as $(\frac{n}{\lambda} + i\frac{1}{r_1\lambda} + [0, r_2 - 1]\tau)_{n \in [1, N]}$ for $i \in [0, r_1 - 1]$. For each $i \in [0, r_1 - 1]$, the packets are forwarded from n -th interval, i.e. $(\frac{n}{\lambda} + i\frac{1}{r_1\lambda} + [0, r_2 - 1]\tau)$, to $n+1$ -th interval, i.e. $(\frac{n+1}{\lambda} + i\frac{1}{r_1\lambda} + [0, r_2 - 1]\tau)$, for $1 \leq n < N$, and from N -th interval to the central controller (Another scheme would be to send in multiple hops from n -th interval to $n+1$ -th interval, i.e. from $(\frac{n}{\lambda} + i\frac{1}{r_1\lambda} + [0, r_2 - 1]\tau)$ to $(\frac{n}{\lambda} + (i+1)\frac{1}{r_1\lambda} + [0, r_2 - 1]\tau)$ for $0 \leq i \leq r_1 - 1$. This however consumes more energy due to the domination of circuit energy over the transmission energy at high sampling rates). The energy consumed in forwarding packets at n -th interval is upper-bounded as

$$e_2 \leq (n-1)(b + \log(r_2))(2e_{elec} + \epsilon_{amp} d_{max}^\alpha), \quad (51)$$

where d_{max} is the maximum distance between a node in n -th interval and a node in $n+1$ -th interval, which is $\frac{1}{\lambda} + \frac{1}{r_1 \lambda 2^{b-1}}$. This energy consumption is distributed among r_2 nodes inside the interval over time such that the energy consumption per node in forwarding is given by $\frac{e_2}{r_2}$.

Finally, the nodes at location $(\frac{n}{\lambda} + i\frac{1}{r_1\lambda} + (m_n^i + 1)\tau)_{n \in [1, N]}$ transmit the level crossing information inside their interval to the right,

$$e_3 = (b + \log(r_2))(e_{elec} + \epsilon_{amp} d_{max}^\alpha). \quad (52)$$

The maximum total energy consumption at a node in n -th interval is then given as

$$e_{tot} = e_s + e_{ADC} + e_1 + \frac{e_2}{r_2} + e_3 \quad (53)$$

$$\begin{aligned} &\leq e_s + e_{ADC} + (b+1)(2e_{elec} + \epsilon_{amp} (\frac{1}{r_1 r_2 \lambda 2^{b-1}})^\alpha) \\ &+ n \frac{(b + \log(r_2))}{r_2} (2e_{elec} + \epsilon_{amp} d_{max}^\alpha) \\ &+ (b + \log(r_2))(e_{elec} + \epsilon_{amp} d_{max}^\alpha) \end{aligned} \quad (54)$$

The energy spent in sensing and at the ADC do not depend on the transmission structure so they are $O(1)$. The transmission energy spent in determining the level crossing is also $O(1)$. Although the total amount of data that should be forwarded by the nodes increases as $O(\log(r_2))$, the load is distributed among r_2 nodes so the energy consumed in forwarding packets is negligible. Sending the level crossing information inside the interval however requires the energy consumption of $O(\log(r_2))$, which cannot be distributed among the nodes. Therefore, e_{tot} is $O(\log(r_2))$ so $O(\log(r))$. The maximum energy consumption in a node per bit gain is therefore $O(1)$.

6 Rate of Data Transmission

The energy consumption is determined by the density of the nodes that determines the precision of the quantization, i.e. r_2 . The density of the nodes that provides diversity for improving the tolerance

to random errors of the ADC on the other hand affects the rate at which the data is delivered in the network. The time duration to determine the level crossing inside each interval is proportional to $(b + 1)r_2$ whereas the time duration required for data forwarding is proportional to $r_1 \log(r_2)$. (It can be easily shown that the same behavior is observed even in multi-hop forwarding strategy.) The bit rate to the central processor is therefore $O(\frac{1}{r^{1/2} \log(r)})$.

7 Fault Tolerance

As stated in [8], the dither-based scheme offers robustness to node failures in terms of a graceful degradation of reconstruction error. If every alternate node fails, the effective node separation would increase to 2τ . This has the same effect as halving the node density r_2 . The same dither function continues to work since it does not depend on r_2 . The nodes will use higher power to determine the threshold crossing inside their interval but the same power to relay the samples to the central controller.

8 Conclusion

We have addressed the effect of the errors occurring at the analog-to-digital converter (ADC), from quantization noise, circuit noise, aperture uncertainty and comparator ambiguity, on the accuracy of sensor field reconstruction. It has previously been shown that PCM-style sampling fails to decrease the quantization error above some finite sampling rate. In this paper, we have demonstrated that the dither-based scheme fails to decrease random errors. We propose an advanced dither-based sampling to reduce both kinds of errors. It is based on distributing the density of the nodes for improving the quantization error and random error. The error of the proposed scheme is $O(\frac{1}{r^{1/2}})$ for oversampling rate r . The maximum energy consumption in a node per bit gain is $O(1)$. Moreover, the bit rate of the scheme is $O(\frac{1}{r^{1/2} \log(r)})$ and it offers robustness to node failures in terms of a graceful degradation of reconstruction error.

The analysis of this paper for 1-D spatially bandlimited sensor field has provided us tremendous insight for the effect of ADC in sampling. In the future, we plan to extend this work for 2-D spatio-temporal sampling. Another direction is to explore the effect of the ADC errors on estimating a relevant function of the sensor field instead of the sensor field itself. We are planning to study the amount of energy that can be saved for specific functions such as calculating the mean or maximum of the field or specific tasks such as detection, classification or localization.

References

- [1] P. Ishwar A. Kumar and K. Ramchandran. On distributed sampling of smooth non-bandlimited fields. In *IPSN*, pages 89–98, 2004.
- [2] W. R. Bennett. Spectra of quantized signals. *Bell System Technical Journal*, 27:446–472, July 1948.
- [3] Z. Cvetkovic. Resilience properties of redundant expansions under additive noise and quantization. *IEEE Transactions on Information Theory*, 49(3):644–656, March 2003.
- [4] Z. Cvetkovic and I. Daubechies. Single-bit oversamples a/d conversion with exponential accuracy in the bit rate. In *Data Compression Conference*, pages 343–352, March 2000.
- [5] Z. Cvetkovic and M. Vetterli. On simple oversampled a/d conversion in $l^2(\mathbb{R})$. *IEEE Transactions on Information Theory*, 47(1):146–154, January 2001.
- [6] Z. Cvetkovic and M. Vetterli. Error-rate characteristics of oversampled analog-to-digital conversion. *IEEE Transactions on Information Theory*, 44(5):1961–1964, September 1998.
- [7] I. Daubechies. *Ten Lectures on Wavelets*. Philadelphia: SIAM.
- [8] A. Kumar P. Ishwar and K. Ramchandran. Distributed sampling for dense sensor networks: A bit-conservation principle. In *IPSN*, pages 17–31, 2003.
- [9] J. Vanderkooy R. A. Wannamaker, S. P. Lipshitz and J. N. Wright. A theory of nonsubtractive dither. *IEEE Transactions on Signal Processing*, 48(2):499–516, February 2000.
- [10] N. T. Thao and M. Vetterli. Deterministic analysis of over-sampled a/d conversion and decoding improvement based on consistent estimates. *IEEE Transactions on Signal Processing*, 42(3):519–530, March 1994.
- [11] R. H. Walden. Analog-to-digital converter survey and analysis. *IEEE Journal on Selected Areas in Communications*, 17(4):539–550, April 1999.